An actin cytoskeleton with evolutionarily conserved functions in the absence of canonical actin-binding proteins

Alexander R. Paredez[a], Zoe June Assaf[a], David Sept[b], Ljudmilla Timofejeva[a,c], Scott C. Dawson[d], Chung-Ju Rachel Wang[a], and W. Z. Cande[a,1]

[a]Department of Molecular and Cell Biology, University of California, Berkeley, CA 94720; [b]Department of Biomedical Engineering and Center for Computational Medicine and Bioinformatics, University of Michigan, Ann Arbor, MI 48109; [c]Department of Gene Technology, Tallinn University of Technology, Tallinn 19086, Estonia; and [d]Department of Microbiology, University of California, Davis, CA 95616

Giardia intestinalis, a human intestinal parasite and member of what is perhaps the earliest-diverging eukaryotic lineage, contains the most divergent eukaryotic actin identified to date and is the first eukaryote known to lack all canonical actin-binding proteins (ABPs). We sought to investigate the properties and functions of the actin cytoskeleton in *Giardia* to determine whether *Giardia* actin (giActin) has reduced or conserved roles in core cellular processes. In vitro polymerization of giActin produced filaments, indicating that this divergent actin is a true filament-forming actin. We generated an anti-giActin antibody to localize giActin throughout the cell cycle. GiActin localized to the cortex, nuclei, internal axonemes, and formed C-shaped filaments along the anterior of the cell and a flagella-bundling helix. These structures were regulated with the cell cycle and in encysting cells giActin was recruited to the Golgi-like cyst wall processing vesicles. Knockdown of giActin demonstrated that giActin functions in cell morphogenesis, membrane trafficking, and cytokinesis. Additionally, *Giardia* contains a single G protein, giRac, which affects the *Giardia* actin cytoskeleton independently of known target ABPs. These results imply that there exist ancestral and perhaps conserved roles for actin in core cellular processes that are independent of canonical ABPs. Of medical significance, the divergent giActin cytoskeleton is essential and commonly used actin-disrupting drugs do not depolymerize giActin structures. Therefore, the giActin cytoskeleton is a promising drug target for treating giardiasis, as we predict drugs that interfere with the *Giardia* actin cytoskeleton will not affect the mammalian host.

cytoskeleton evolution | actin protofilaments | MreB | endocytosis | Rac

The protozoan intestinal parasite *Giardia intestinalis* is a major cause of waterborne diarrheal disease throughout the world. The lineage containing *Giardia* has been controversially placed as the earliest to diverge from other eukaryotes (1–4, reviewed in ref. 5). The *Giardia* genome contains homologs of most conserved microtubule cytoskeleton components; however, it contains only a single divergent actin gene (giActin) with an average 58% identity to actin from other species (2, 6). *Giardia* lacks the core set of actin-binding proteins (ABPs), including the ARP2/3 complex, formin, myosin, and others previously thought common to all extant eukaryotes (2, 7, 8). Whether *Giardia* once possessed the core set of ABPs and lost them or whether it diverged from the eukaryotic lineage before the core set of ABPs evolved remains an open question. In either case, *Giardia* is the first example of a eukaryote that lacks all canonical ABPs. Here we explore *Giardia* actin function in the absence of core ABPs.

Results

GiActin Is a Divergent Filament-Forming Actin.
We first explored the structural implications of the high divergence of giActin by mapping the *Giardia* sequence onto a protomer from the Oda et al. fibrous (F)-actin structure (9). Of the 155 substitutions between giActin and muscle actin, 48 are highly nonconservative, including six at filament contact points involving both the DNaseI loop (residues 39–47) and hydrophobic plug (residues 266–269) (Fig. 1 *A* and *B*). The hydrophobic plug has been implicated in coordinating interactions between three actin subunits (10), whereas the DNaseI loop coordinates monomer–monomer contacts and contributes to filament stability. Point mutations in the hydrophobic plug of conventional actin result in destabilized and aberrant filaments (kinks and bends) (11, 12), and notably, the sequence ^{266}FIGM^{269} in muscle actin is ^{266}LNNS^{269} in giActin. These substitutions in domains important for F-actin function represent major differences between giActin and muscle actin and imply altered filament properties.

The divergent sequence of giActin called into question whether giActin could form filaments. To test the filament-forming ability of giActin, we purified giActin and found that the protein could be selectively pelleted under standard filament-forming conditions. Functional protein selected by cycling between monomers and filaments was analyzed by electron microscopy. GiActin filaments were shorter and had greater curvature than filaments formed by rabbit muscle actin (Fig. 1 *C–E* and Fig. S1). In addition to conventional filaments with an approximate width of 7 nm, we observed filaments with half this diameter, which likely represent protofilaments and occasionally we observe thinner filaments associating/dissociating from thicker filaments (Fig. 1*E*). Although protofilaments have not been observed for other eukaryotic actins, they have been observed for the bacterial actin homolog MreB (13, 14).

GiActin Forms Discrete Structures.
Next, we sought to determine the localization of actin in *Giardia* cells. Due to the divergence of *Giardia*, we raised polyclonal antibodies against full-length giActin, obtaining two independent antibodies that recognize identical structures in trophozoites as well as a single band at the expected molecular weight in *Giardia* cell extracts (Fig. 2*A*). The *Giardia* life cycle consists of two main stages: the flagellated trophozoite, which colonizes the small intestine, and the infectious cyst. Actin localization in *Giardia* trophozoites revealed enrichment of actin at the cortex, in both nuclei, and in association with the internal axonemes and flagella (Fig. 2 *B* and *C*). Labeling of the external flagella, where actin is a known component of the flagellar inner dynein arms (15–17), had a punctate
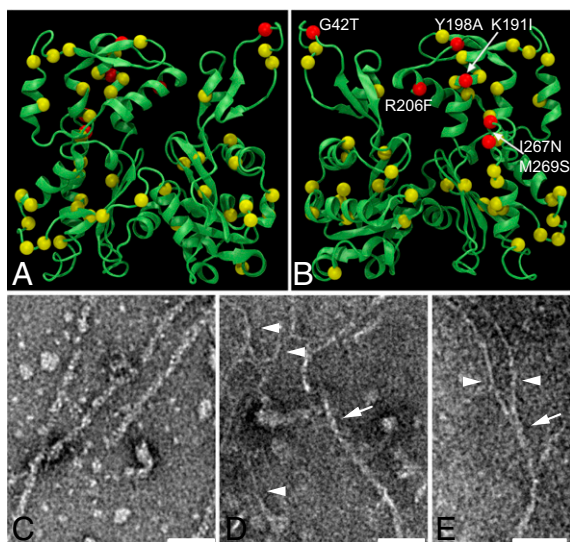
CELL BIOLOGY

Fig. 1. Divergent GiActin forms filaments. (*A* and *B*) Front and back views of giActin mapped on the F-actin structure with 48 nonconservative substitutions indicated in yellow and red. Nonconservative substitutions at filament contact points are in red. Note the substitutions in the DNaseI loop (residues 39–47) and the hydrophobic plug (residues 266–269). (*C–E*) TEM of negative-stained (*C*) rabbit actin and (*D* and *E*) giActin. Arrows point to ~7-nm filaments; arrowhead points to ~3.5-nm filaments. (Scale bar, 50 nm.)

appearance, whereas the internal axonemes were covered in dispersed label. C-shaped actin filaments perpendicular to the internal axonemes of the anterior flagella appeared in association with the membrane protrusion known as the ventrolateral flange, and an unusual helix of actin was observed to envelope the caudal flagella pair (Fig. 2 *B* and *C* and Movies S1 and S2 and Fig. S2). Using 3D structured illumination light microscopy (3D-SIM), a new method of super resolution light microcopy

(18), we found that in addition to the thicker filaments at the anterior, thin C-shaped filaments are located all along the periphery of trophozoites, suggesting the filaments at the anterior are bundled (Fig. S2). We were also able to resolve a regular zig-zag pattern of actin within the axonemes of the flagella (Fig. S2). We observed filamentous actin structures within *Giardia*, and in contrast to previous studies using heterologous antibodies of unknown specificity (19, 20), we did not observe pronounced actin staining of the ventral disk, a microtubule structure used for parasite attachment.

Actin and tubulin localization were followed throughout the cell cycle and encystation to determine whether giActin formed stage-dependent structures. During mitosis, the anterior, dorsal, and ventral flagella pairs (Fig. 2*B*) are repositioned by an unknown mechanism (21, 22). Coincidentally, a cloud of actin was observed around the corresponding internal axonemes. Before axoneme repositioning, the C-shaped actin filaments normally associated with the anterior flagella are disassembled and then reassembled after flagellar repositioning and before cytokinesis proceeds (Fig. 2*B*). Cyst formation requires the production and secretion of massive amounts of cyst wall protein (CWP). *Giardia* does not contain a true Golgi apparatus; yet, CWP is processed in encystation-specific vesicles (ESVs), where, like in Golgi, cargo proteins undergo delayed secretion to allow for processing (23). Interestingly, we found that giActin is associated with mature ESVs, similar to the manner in which actin associates with Golgi in other eukaryotes (Fig. 2*D*). Thus, giActin displayed dynamic changes in organization that were regulated in a stage-dependent manner, suggesting *Giardia* has the ability to regulate filament formation.

In most eukaryotes the ARP2/3 complex is central to regulating actin function (24). Although components of the ARP2/3 complex are not found in *Giardia*, there are three actin-related proteins (ARPs) in the *Giardia* genome. We performed maximum likelihood phylogenetic analysis on the *Giardia* ARPs and were unable to group these proteins with any known ARP subfamily. N-terminal GFP fusions to the three giARPs localized to
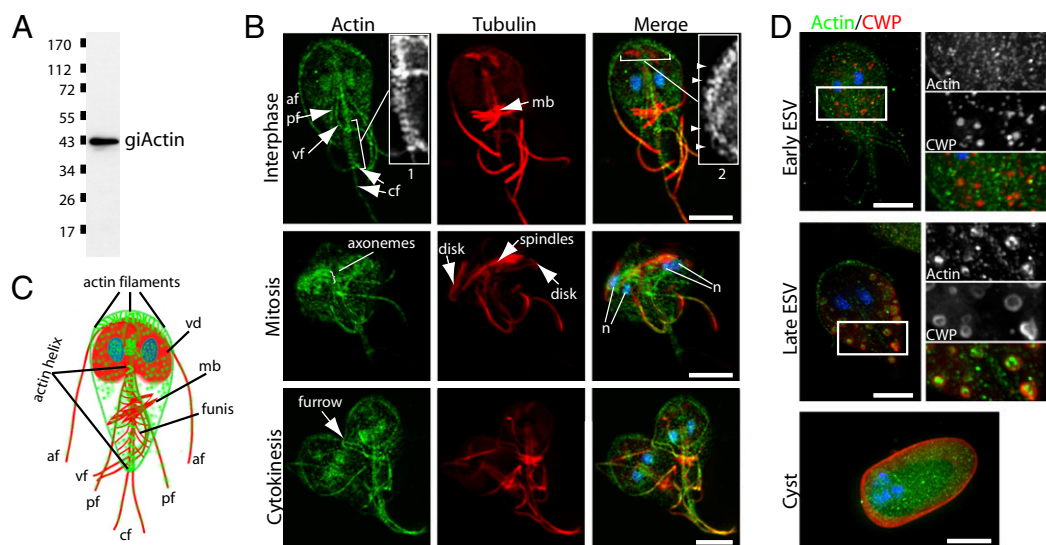

Fig. 2. GiActin forms stage-specific structures. (*A*) Anti-giActin Western blot against total *Giardia* extract. (*B*) Immunofluorescence labeling of actin (green), tubulin (red), and DNA (blue) in trophozoites. Actin localizes to the cortex, the two nuclei, and all axonemes. An actin helix bundles the caudal flagella pair (cf) *Inset* 1, and short filaments are visible along the anterior flagella (af) *Inset* 2 (arrowheads). Note the repositioning of the af, ventral flagella (vf), and posterior flagella (pf) and enrichment of actin during mitosis. (*C*) Diagram of actin (green) and microtubule (red) cytoskeletons in trophozoites, including eight flagella, a ventral disk (vd) (parasite attachment), the median body (mb) (likely a microtubule reservoir), and the funis (rib-like microtubule structure). (*D*) Localization of actin (green) and cyst wall protein (CWP) (red) in encysting trophozoites. Note the recruitment of actin to mature encystation-specific vesicles ESVs. (Scale bar, 5 μm.)

the nuclei (Fig. S3), where actin and the ARPs are thought to have ancient nuclear functions (25). Thus, the *Giardia* ARPs are unlikely involved in extranuclear actin regulation.

Others (26) have reported actin localization in *Giardia* by phalloidin staining, which appears diffuse throughout the cell and enriched in the median body (a *Giardia*-specific microtubule structure). Our efforts to stain *Giardia* trophozoites with fluorescent phalloidin failed to detect any signal above background (Fig. S4A). In light of the major differences in staining patterns between phalloidin and our *Giardia*-specific giActin antibodies, we contend that any observed phalloidin staining is background, and phalloidin does not actually recognize giActin. Nevertheless, to test in a controlled manner the ability of phalloidin to recognize giActin, we expressed giActin in mammalian COS-7 cells and stained the cells with both phalloidin and our anti-giActin antibody. The failure of phalloidin to recognize giActin, and our antibody to recognize metazoan actin, allowed us to differentiate between giActin and mammalian actin. The two proteins did not colocalize within discrete filaments (Fig. 3A). Interestingly, giActin did form ring and helix-like structures, consistent with the actin helices observed in trophozoites, suggesting helix formation is an innate property of giActin (Fig. 3A and Movie S3). In addition, giActin could be observed at ruffled cell edges, reminiscent of a Rac-signaling response (27) (Fig. 3B). Consistent with *Giardia* being an early diverging eukaryote, its genome contains a single Rac homolog (28) and Rac is thought to be the founding member of the Rho family of small G proteins (29). To test for a conserved actin-signaling response in *Giardia*, we constructed a constitutive active Q74L giRac (equivalent to Q61L Rac1) (30). Indeed Q74L giRac caused cellular disorganization, nuclear missegregation, large vesicle formation, and actin levels to increase (Fig. 3C).

GiActin Functions in Core Cellular Processes Without Core ABPs. Cytochalasin and latrunculin have been used previously to probe actin function in *Giardia* often with conflicting results; moreover, in those studies, either no attempt was made to monitor actin distribution during the experiment, or heterologous antibodies (without controls) or phalloidin were used (20, 26, reviewed in ref. 8). We tested the ability of latrunculin B and cytochalasin D to disrupt giActin localization and cellular organization using concentrations ranging from 10 to 100 μM. However, even after treatment with 100 μM cytochalasin D for 24 h, only 10% (18/178) of the treated cells displayed abnormal morphologies (similar results for latrunculin B), whereas the remaining cells had normal actin distributions (Fig. S4B). The crystal structures of actin bound to cytochalasin D and latrunculin B are solved, so we examined the drug-binding pockets of giActin and found several substitutions consistent with reduced drug efficacy (31, 32) (Fig. S4 C–E).

Therefore, as an alternative to drug treatment, we knocked down actin expression using translation-blocking morpholinos (33). We examined actin levels at 6, 12, and 24 h after electroporation with 100 μM anti-giActin morpholino or a 5-bp mismatch control (Fig. 4 A and B). Morphological phenotypes were detectable within 6 h of electroporation, giActin levels were measurably reduced by 12 h, and a maximum knockdown of nearly 80% was reached after 24 h (approximately four cell cycles).

Actin and tubulin staining revealed several defects in the morphology of actin knockdown trophozoites (Fig. 4C and Fig. S5). Severe defects included gross morphological changes, misplacement of the flagella, missegregation of nuclei, and cytokinesis defects resulting in cells with 1 nucleus (wild type has 2 nuclei) to 10 nuclei (Fig. 4 C and D). Subtle phenotypes included reduced cortical actin and splaying of the caudal flagella pair, highlighting the structural importance of the actin helix surrounding the caudal flagella. Additionally, cells that appeared otherwise
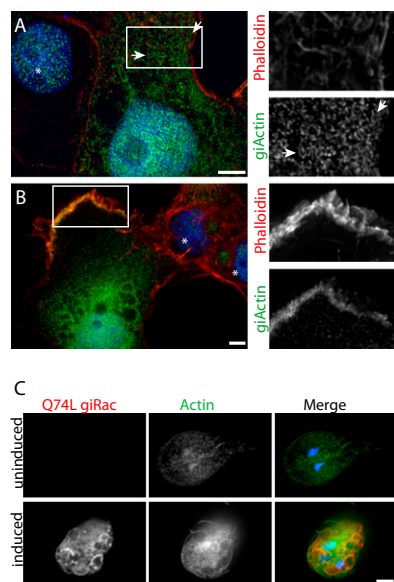
Fig. 3. GiActin forms helical structures in COS-7 cells and responds to Rac signaling. (A) GiActin was transiently transfected into COS-7 cells. GiActin, detected using giActin-specific antibodies is green, phalloidin staining is red (mammalian actin), and DNA is blue. Arrows indicate helices. Asterisk marks untransfected cell, to indicate background staining levels. Note giActin and phalloidin do not copolymerize. (B) GiActin is enriched at ruffled cell edge. (C) Expression of Q74L HA-giRac disrupts cell morphology, causes DNA missegregation, induces vesicle formation, and increases actin levels. (Scale bar, 5 μm.)
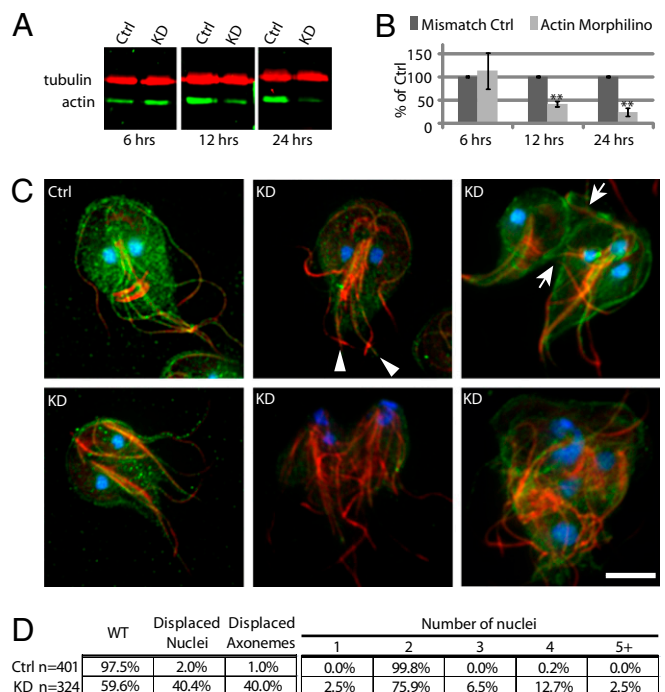
Fig. 4. GiActin functions in cell shape, polarity, and cytokinesis. (A) Western blot of morpholino-treated cells, probed with anti-giActin (green) and anti-tubulin (red) antibodies. (B) Quantification of actin knockdown. n = 3, error bars are SD, **$P < 0.01$. (C) Immunofluorescent images of mismatch control cell versus actin knockdown phenotypes. Arrowheads indicate unbundled caudal flagella; arrows indicate failed cytokinesis. (D) Quantification of observed phenotypes. (Scale bar, 5 μm.)

	WT	Displaced Nuclei	Displaced Axonemes	Number of nuclei				
				1	2	3	4	5+
Ctrl n=401	97.5%	2.0%	1.0%	0.0%	99.8%	0.0%	0.2%	0.0%
KD n=324	59.6%	40.4%	40.0%	2.5%	75.9%	6.5%	12.7%	2.5%

normal would frequently have one or more mispositioned nuclei. This phenotype was observed in 2% of the mismatch control population, compared with 40% in the knockdown population (Fig. 4D). All of these defects are consistent with actin playing a role in nuclear positioning, axonemal positioning, cell polarity, and cytokinesis.

The role of giActin in cytokinesis is perplexing, given that *Giardia* lacks a contractile ring. One possibility is that giActin contributes to membrane/vesicle trafficking, which is essential for cytokinesis in plants and animals (reviewed in ref. 34). Therefore, we examined the ability of actin knockdown cells to perform fluid-phase endocytosis (Fig. 5A). Twenty-five minutes after the addition of Lucifer yellow, the fluorescence of the actin knockdown population was $124 \pm 8\%$ ($n = 3$, 10,000 cells per experiment, SD) of the control and increased to $172 \pm 20\%$ after 1 h, indicating that giActin is not required for fluid-phase endocytosis. To test whether the increased levels of Lucifer yellow were due to a downstream processing defect, we performed pulse-chase experiments. After a 40-min chase, $30.4 \pm 8.6\%$ ($n = 3$, 10,000 cells per experiment, SD) of the actin knockdown cells remained positive for Lucifer yellow, versus $3.2 \pm 1\%$ in the control cells (Fig. S6). This result indicates that actin participates in the clearing, possibly through bulk secretion, but not the uptake of Lucifer yellow.

We also tested whether giActin plays a role in receptor-mediated endocytosis. In *Giardia*, low-density lipoprotein (LDL) is taken up via a clathrin-dependent pathway (35, 36). As with giActin, inhibition of the *Giardia* clathrin-mediated endocytosis pathway does not prevent the uptake of fluid-phase markers (36). We analyzed the ability of actin knockdown cells to endocytose fluorescent Bodipy-LDL. We found a $25.8 \pm 4.3\%$ ($n = 3$,

10,000 cells per experiment, SD) decrease in fluorescence, indicating that giActin plays a role in this clathrin-mediated process (Fig. 5B).

GiActin Is Required for Cyst Formation. We have shown that giActin is associated with the Golgi-like ESVs (Fig. 2D), where the trafficking of CWP is thought to involve clathrin and dynamin (37). To test the role of giActin in CWP trafficking, we encysted actin knockdown cultures. Surprisingly, these cultures displayed a 2.2-fold increase in cyst number. Because *Giardia* encystation can be triggered by lipoprotein deprivation (38), the function of actin in LDL uptake is consistent with reduced perception of LDL and the increased encystation efficiency of actin knockdown cultures. To assay the integrity of actin knockdown cysts, we treated encysted cultures with water to lyse any nonencysted cells and then measured cyst wall integrity/viability by staining with trypan blue. Cyst viability was reduced to $17.6 \pm 2.4\%$ ($n = 3$, SD) in the actin knockdown population, versus $38.8 \pm 5.1\%$ for the control, suggesting that giActin indeed plays a role in CWP maturation and/or trafficking (Fig. 5C). Although the reductions in LDL uptake and cyst viability shown in Fig. 5 are statistically significant (*t* test), actin silencing is incomplete (40% of knockdown cells have defects, Fig. 4D). Individual cells exhibit varied levels of actin knockdown; therefore, our quantification of giActin's contribution to endocytosis and trafficking in whole populations is likely an underestimate of its actual contribution. The contrast is apparent in Fig. 5B, which shows the typical fluorescence of a morphologically defective knockdown versus a control trophozoite.

Discussion

G. intestinalis is a divergent eukaryote lacking all core ABPs and possessing the most divergent actin studied to date. Nevertheless, there are other eukaryotes that lack at least some core ABPs. For example, *Trichomonas* and *Cyanidioschyzon* lack myosin, whereas the Trypanosomes are missing nucleation-promoting factors, actin cross-linking proteins, and the dynactin complex (39–41). *Spironucleus vortens*, a fish commensal and a close relative of *Giardia* (both of the order Diplomonadida), is the only other example of a eukaryote lacking the core set of ABPs. Like *Giardia*, searches for cytoskeletal components within the *Spironucleus* genome readily identify microtubule cytoskeleton components and actin, yet fail to identify any conserved ABPs (Table S1). That a closely related and free-living diplomonad also lacks the core set of ABPs suggests that *Giardia*'s divergent actin and lack of ABPs are not simply a result of its parasitic lifestyle.

Given the lack of known actin-binding proteins in *Giardia*, we expected to find reduced or limited functions for actin, yet we have shown that giActin functions in conserved actin-based processes. Table 1 summarizes the actin functions we have identified and compares the components known to function in these processes in other eukaryotes with those identifiable in *Giardia*. Whether the regulation we associate with actin in other eukaryotes was built upon a system like in *Giardia* or the diplomonad actin cytoskeleton was derived from a more canonical one remains unclear. However, the specific recruitment and regulation of giActin throughout the *Giardia* life cycle argues for the presence of some as-yet-unidentified regulatory proteins.

Intriguingly, the *Giardia* genome contains a similar number of genes as yeast; however, many of the *Giardia* pathways appear to be simplified in terms of having fewer and more basic components (2). With respect to the actin cytoskeleton, it seems unlikely that the diplomonads would lose all of the actin regulatory proteins used by other eukaryotes and then reinvent mechanisms to recruit actin to core cellular functions. Therefore, we favor the view that the diplomonads never possessed the core set of ABPs. Working out the molecular mechanisms for giActin function in these core cellular processes may provide insight into the
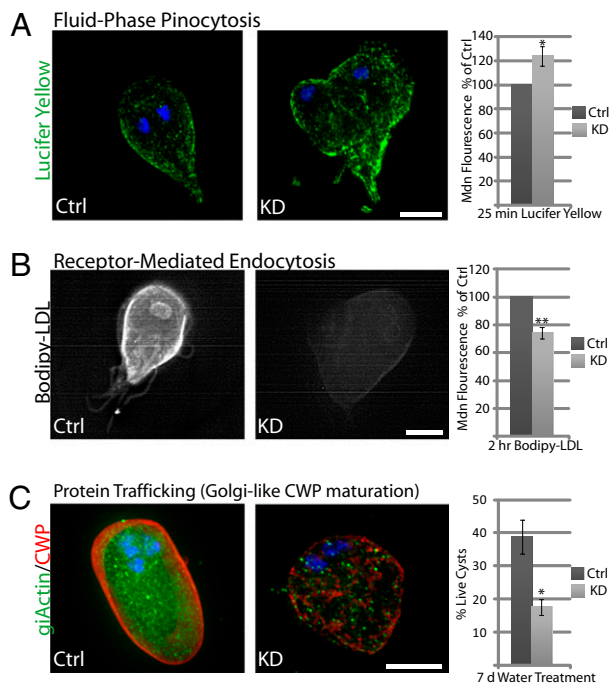

Fig. 5. GiActin knockdown reveals functions in endocytosis and trafficking. (A) Trophozoites were exposed to the fluid-phase marker Lucifer yellow (green), and the DNA was stained using DAPI (blue). Quantification by flow cytometry indicates that giActin is not required for Lucifer yellow uptake. (B) Receptor-mediated endocytosis of Bodipy-LDL is inhibited by actin knockdown. (C) Immunofluorescence staining shows that Golgi-like processing of CWP (red) requires actin (green). Quantification indicates reduced cyst viability in actin knockdown cells. $n = 3$ and error bars are SD; *$P < 0.05$, **$P < 0.01$. (Scale bar, 5 μm.)

Table 1. In vivo giActin function versus known components

Function	*Giardia*	Other eukaryotes
Actin nucleation (24)	?*	Arp2/3, formin, spire, Cobl, leiomodin
Actin signaling (50)	giRac	Rho, Rac, Cdc42
Downstream of G protein (50)	PAK, ?	PAK, cofilin, myosin, formin, Arp2/3, gelsolin
Endocytosis (44)	Clathrin, dynamin, ?	Clathrin, dynamin, Wasp, Wasp regulators, Arp2/3, Arp2/3 activators, myosin, fimbrin, Abp1, capping proteins
Cytokinesis (contractile) (51)	None	Rho, myosin, formin, annilin, cofilin, capping protein
Cytokinesis (vesicular delivery, midbody phragmoplast) (34)	Dynamin, Sec1, Snap, CDC48, Rab11	Dynamin, Sec1, Snap25, CDC48p, Rab11
Flagella (inner arm dynein) (17)	giActin, p28, centrin	Actin, p28, centrin

GiActin forms stage-specific structures and performs core cellular processes. Conserved components found in *Giardia* and other eukaryotes are listed.
*The placement of distinct organized giActin structures suggests the presence of a protein or protein complex that controls giActin nucleation.

requirements for actin in these processes and possibly reveal mechanisms of actin regulation that were lost or are deeply buried in other eukaryotes.

Rac signaling of the actin cytoskeleton appears to be conserved from *Giardia* to man, but the ABPs currently known to link Rac to actin are not found in *Giardia*. The response of giActin to Rac signaling in *Giardia* and the localization of giActin to ruffled cell edges of transgenic COS-7 cells, suggest the existence of a conserved Rac-signaling mechanism in *Giardia* that may also be functioning in mammalian cells. Because small G protein signaling is simpler in *Giardia* (i.e., there is no Rho or CDC42 and only 3 Rho Gap proteins versus over 70 in mammalian cells) (42), it may be easier to work out the fundamental principles of G protein signaling in *Giardia* than in more complex systems.

Membrane/vesicle trafficking is another area where studying basic cell biology in *Giardia* could lead to the discovery of key universal requirements. We have shown that actin is involved in the trafficking of CWP, clathrin-mediated endocytosis, and cytokinesis that is likely mediated by trafficking. There are differing requirements for actin in endocytosis between eukaryotes as close as yeast and man (43); however, even in *Giardia*, there is a role for actin in clathrin-mediated endocytosis. Although the list of components differs between yeast and mammalian systems (44), there are some common components, whereas *Giardia* has almost none of these proteins (Table 1). Therefore, studying such processes in a simplified system like *Giardia* can help define what is at the core of these processes in terms of basic mechanistic requirements.

Regardless of whether the actin regulatory proteins are conserved in all eukaryotes or are *Giardia* specific, their identification will provide evolutionary insight and possibly novel modes of actin regulation. Thus, far, our homology searches have only identified the actin-binding proteins P28/IDA4 and centrin, which are components of the inner dynein arm of flagella (17). These proteins are thought to bind monomeric actin in a complex rather than regulate actin dynamics; however, their conservation in flagellates from *Giardia* to man indicates that actin function in the flagella is ancestral (Fig. S2). The function of giActin in other essential cellular processes predicts divergent or novel actin regulators, making the actin cytoskeleton a promising drug target, as we predict some drugs that interfere with the *Giardia* actin cytoskeleton will not affect the mammalian host. Our observation that giActin forms protofilaments and helical structures like the bacterial homolog of actin, MreB, may have evolutionary implications (45). If *Giardia* truly belongs to the earliest diverging eukaryotic lineage, perhaps giActin and its predicted novel ABPs represent evolutionary intermediates. Only by identifying giActin interactors and analyzing the genomes of additional diverse species, will we gain further insight into the evolution of the actin cytoskeleton.

Materials and Methods

Native Actin Purification. Rabbit muscle actin was provided by M. Welch (University of California, Berkeley). GiActin (ORF GL50803_40817) was cloned into p10.pApolh-2.IKE-EE (T. Ohkawa, University of California, Berkeley) between NdeI and XhoI. Recombinant virus was generated using BestBac linearized DNA (Expression Systems). SF9 cells were transfected at 2 multiplicity of infection (MOI) and cell pellets were harvested 3 d postinfection. Cells were lysed by sonication in 20 mM Tris 8.0, 350 mM NaCl, 0.2 mM CaCl2, 0.2 mM ATP, 0.02% NaN3, and 2 mM 2-mercaptoethanol. Cleared 6× His-giActin lysate was bound to NiNTA agarose (Qiagen) and washed with G-buffer plus: 10 mM imidazole; 500 mM NaCL, 5 mM imidazole; 500 mM NaCL 5 mM imidazole, and then eluted with G-buffer plus 250 mM imidazole. 6× His-giActin was then dialyzed against G-buffer and the His tag was liberated with Actev protease (Invitrogen). Then the tag and protease were absorbed against NiNTA beads and the actin prep was cleared at 100,000 × g. Subsequently, giActin was polymerized by adding 10× KMEI (800 mM KCL, 2 mM MgCl, 2 mM EDTA, 10 mM Imidazole pH 7) and pelleted at 100,000 × g. The giActin pellet was resuspended in G-buffer and quantified by comparison with known quantities of rabbit muscle actin.

Denatured Actin Purification and Antibody Production. GiActin was cloned into pET30C(+) between EcoRV and NotI and expressed in BL21 DE3 cells. The protein was purified with NiNTA agarose following the Qiagen Expressionist protocol for denaturing purification. Two rabbits from Covance Research Products were selected without background and antibodies were generated with their 118-d protocol.

Electron Microscopy of Actin Filaments. Purified giActin or rabbit muscle actin was diluted to 2 μM in G-buffer and induced to polymerize using 10× KMEI. After 30 min at room temperature (RT), the reactions were iced and the polymerized actin was absorbed onto freshly glow-discharged formvar-coated Cu grids. The excess was wicked off and the grids were stained with 1% uranyl acetate for 5 min.

***Giardia* ARPs.** The tetracycline-inducible pTetGFPC.pac vector (46) was modified with a GLY-SER linker suitable for N-terminal fusions to make pTetGFPN.pac. Subsequently the three *Giardia* ARPs (ORF GL50803_15113, GL50803_16172, and GL50803_11039) were inserted between BstBI and NotI restriction sites.

Fixation and Fluorescence Microscopy. Fixation conditions were adapted from ref. 47. Cells were pelleted at 500 × g at RT and the pellet was fixed in PME (100 mM Pipes pH 7.0, 5 mM EGTA, 10 mM MgSo4) plus 2% paraformaldehyde, 100 μM MBS, 100 μM EGS (Pierce), and 0.025% Triton X-100 for 30 min at 37 °C. Cells were washed in PME and then adhered to coverslips. The cells were washed again and permeabilized with 0.1% Triton X-100 for 10 min. After two washes with PME, the cells were blocked in PMEBALG for 30 min (PME + 1% BSA, 0.1% NaN3, 100 mM lysine, 0.5% cold water fish skin gelatin (Sigma). Rabbit anti-giActin antibody 28PB+1 and mouse monoclonal anti α-tubulin antibody TAT1 (48) were both diluted 1:125 in PEMBALG and

CELL BIOLOGY

incubated overnight. After three washes with PME + 0.05% Triton X-100, Alexa 488 goat antirabbit and Alexa 555 goat antimouse (Molecular Probes) secondary antibodies were diluted 1:125 in PEMBALG and incubated for 1 h. After three washes with PME + 0.05% Triton X-100, the coverslips were mounted with Prolong antifade plus DAPI (Molecular Probes). Fluorescence deconvolution microscopy images were collected as in ref. 22. 3D-SIM images were aquired as described in ref. 18.

Fluid-Phase Endocytosis Assay. One milliliter of cells (2×10^6) was incubated with 5 mg/mL Lucifer yellow CH lithium salt (Invitrogen). After 25 min, the cells were iced and washed two times in cold HBS (5 mM glucose, 20 mM Hepes, 5 mM KCl, 135 mM NaCl, 0.75 mM NA_2HPO_4, pH 7.0). A final wash was performed in cold stripping buffer (50 mM Mes, 200 mM NaCl, pH 5.0), and cells were fixed without MBS and EGS. The cells were washed two times in PEM and quantified on a Beckman-Coulter EPICS XL flow cytometer. For pulse-chase experiments cells were washed after 1 h and immediately quantified on the flow cytometer. Histogram overlays were created using WinMDI (Salk Institute).

Receptor-Mediated Endocytosis Assay. Five hours after morpholino treatment, TYDK media was exchanged for lipoprotein-deficient TYDK (standard serum substituted with 5% bovine BTI lipoprotein-deficient serum, Biomedical Technologies). BODIPY FL LDL (Invitrogen) endocytosis assays were performed 18 h after morpholino treatment as in ref. 36 and the fluorescence quantified by flow cytometry.

Encystation and Viability Assay. Trophozoites were encysted 6 h post-morpholino treatment as in ref. 49. Seven days after water treatment, cysts were stained with trypan blue and counted on a hemocytometer.

Construction of Q74L HA-giRac. GiRac (orf GL50803_8496) was amplified by sewing PCR using Rac_NF + Rac_CA-R and Rac_CR + Rac_CA-R to introduce the Q74L mutation and the PCR product was inserted between AscI and NotI of pTet-3HA.pac.

1. Ciccarelli FD, et al. (2006) Toward automatic reconstruction of a highly resolved tree of life. *Science* 311:1283–1287.
2. Morrison HG, et al. (2007) Genomic minimalism in the early diverging intestinal parasite *Giardia* lamblia. *Science* 317:1921–1926.
3. Cavalier-Smith T (2002) The phagotrophic origin of eukaryotes and phylogenetic classification of Protozoa. *Int J Syst Evol Microbiol* 52:297–354.
4. Hampl V, et al. (2009) Phylogenomic analyses support the monophyly of Excavata and resolve relationships among eukaryotic "supergroups.". *Proc Natl Acad Sci USA* 106:3859–3864.
5. Fritz-Laylin LK, et al. (2010) The genome of Naegleria gruberi illuminates early eukaryotic versatility. *Cell* 140:631–642.
6. Drouin G, Moniz de Sá M, Zuker M (1995) The *Giardia* lamblia actin gene and the phylogeny of eukaryotes. *J Mol Evol* 41:841–849.
7. Pollard TD (2003) The cytoskeleton, cellular motility and the reductionist agenda. *Nature* 422:741–745.
8. Elmendorf HG, Dawson SC, McCaffery JM (2003) The cytoskeleton of *Giardia* lamblia. *Int J Parasitol* 33:3–28.
9. Oda T, Iwasa M, Aihara T, Maéda Y, Narita A (2009) The nature of the globular- to fibrous-actin transition. *Nature* 457:441–445.
10. Holmes KC, Popp D, Gebhard W, Kabsch W (1990) Atomic model of the actin filament. *Nature* 347:44–49.
11. Chen X, Cook RK, Rubenstein PA (1993) Yeast actin with a mutation in the "hydrophobic plug" between subdomains 3 and 4 (L266D) displays a cold-sensitive polymerization defect. *J Cell Biol* 123:1185–1195.
12. Orlova A, et al. (2004) Actin-destabilizing factors disrupt filaments by means of a time reversal of polymerization. *Proc Natl Acad Sci USA* 101:17664–17668.
13. Popp D, et al. (2010) Filament structure, organization, and dynamics in MreB sheets. *J Biol Chem* 285:15858–15865.
14. van den Ent F, Amos LA, Löwe J (2001) Prokaryotic origin of the actin cytoskeleton. *Nature* 413:39–44.
15. Bui KH, Sakakibara H, Movassagh T, Oiwa K, Ishikawa T (2008) Molecular architecture of inner dynein arms in situ in Chlamydomonas reinhardtii flagella. *J Cell Biol* 183:923–932.
16. Piperno G, Luck DJL (1979) An actin-like protein is a component of axonemes from Chlamydomonas flagella. *J Biol Chem* 254:2187–2190.
17. Yanagisawa HA, Kamiya R (2001) Association between actin and light chains in Chlamydomonas flagellar inner-arm dyneins. *Biochem Biophys Res Commun* 288:443–447.
18. Wang CJR, Carlton PM, Golubovskaya IN, Cande WZ (2009) Interlock formation and coiling of meiotic chromosome axes during synapsis. *Genetics* 183:905–915.
19. Feely DE, Schollmeyer JV, Erlandsen SL (1982) *Giardia* spp.: Distribution of contractile proteins in the attachment organelle. *Exp Parasitol* 53:145–154.
20. Corrêa G, Benchimol M (2006) *Giardia* lamblia behavior under cytochalasins treatment. *Parasitol Res* 98:250–256.
21. Nohynková E, Tumová P, Kulda J (2006) Cell division of *Giardia* intestinalis: Flagellar developmental cycle involves transformation and exchange of flagella between mastigonts of a diplomonad cell. *Eukaryot Cell* 5:753–761.
22. Sagolla MS, Dawson SC, Mancuso JJ, Cande WZ (2006) Three-dimensional analysis of mitosis and cytokinesis in the binucleate parasite *Giardia* intestinalis. *J Cell Sci* 119:4889–4900.
23. Marti M, et al. (2003) An ancestral secretory apparatus in the protozoan parasite *Giardia* intestinalis. *J Biol Chem* 278:24837–24848.
24. Campellone KG, Welch MD (2010) A nucleator arms race: Cellular control of actin assembly. *Nat Rev Mol Cell Biol* 11:237–251.
25. Blessing CA, Ugrinova GT, Goodson HV (2004) Actin and ARPs: Action in the nucleus. *Trends Cell Biol* 14:435–442.
26. Castillo-Romero A, et al. (2009) Participation of actin on *Giardia* lamblia growth and encystation. *PLoS ONE* 4:e7156.
27. Ridley AJ, Paterson HF, Johnston CL, Diekmann D, Hall A (1992) The small GTP-binding protein rac regulates growth factor-induced membrane ruffling. *Cell* 70:401–410.
28. Brembu T, Winge P, Bones AM, Yang ZB (2006) A RHOse by any other name: A comparative analysis of animal and plant Rho GTPases. *Cell Res* 16:435–445.
29. Boureux A, Vignal E, Faure S, Fort P (2007) Evolution of the Rho family of ras-like GTPases in eukaryotes. *Mol Biol Evol* 24:203–216.
30. Xu XM, Barry DC, Settleman J, Schwartz MA, Bokoch GM (1994) Differing structural requirements for GTPase-activating protein responsiveness and NADPH oxidase activation by Rac. *J Biol Chem* 269:23569–23574.
31. Morton WM, Ayscough KR, McLaughlin PJ (2000) Latrunculin alters the actin-monomer subunit interface to prevent polymerization. *Nat Cell Biol* 2:376–378.
32. Nair UB, et al. (2008) Crystal structures of monomeric actin bound to cytochalasin D. *J Mol Biol* 384:848–864.
33. Carpenter ML, Cande WZ (2009) Using morpholinos for gene knockdown in *Giardia* intestinalis. *Eukaryot Cell* 8:916–919.
34. Baluska F, Menzel D, Barlow PW (2006) Cytokinesis in plant and animal cells: endosomes 'shut the door.' *Dev Biol* 294:1–10.
35. Lujan HD, Mowatt MR, Nash TE (1996) Lipid requirements and lipid uptake by *Giardia* lamblia trophozoites in culture. *J Eukaryot Microbiol* 43:237–242.
36. Rivero MR, et al. (2010) Adaptor protein 2 regulates receptor-mediated endocytosis and cyst formation in *Giardia* lamblia. *Biochem J* 428:33–45.
37. Gaechter V, Schraner E, Wild P, Hehl AB (2008) The single dynamin family protein in the primitive protozoan *Giardia* lamblia is essential for stage conversion and endocytic transport. *Traffic* 9:57–71.
38. Luján HD, Mowatt MR, Byrd LG, Nash TE (1996) Cholesterol starvation induces differentiation of the intestinal parasite *Giardia* lamblia. *Proc Natl Acad Sci USA* 93:7628–7633.
39. Berriman M, et al. (2005) The genome of the African trypanosome Trypanosoma brucei. *Science* 309:416–422.
40. Carlton JM, et al. (2007) Draft genome sequence of the sexually transmitted pathogen *Trichomonas vaginalis*. *Science* 315:207–212.
41. Matsuzaki M, et al. (2004) Genome sequence of the ultrasmall unicellular red alga Cyanidioschyzon merolae 10D. *Nature* 428:653–657.
42. Tcherkezian J, Lamarche-Vane N (2007) Current knowledge of the large RhoGAP family of proteins. *Biol Cell* 99:67–86.
43. Aghamohammadzadeh S, Ayscough KR (2009) Differential requirements for actin during yeast and mammalian endocytosis. *Nat Cell Biol* 11:1039–1042.
44. Kaksonen M, Toret CP, Drubin DG (2006) Harnessing actin dynamics for clathrin-mediated endocytosis. *Nat Rev Mol Cell Biol* 7:404–414.
45. Jones LJF, Carballido-López R, Errington J (2001) Control of cell shape in bacteria: Helical, actin-like filaments in Bacillus subtilis. *Cell* 104:913–922.
46. Dawson SC, et al. (2007) Kinesin-13 regulates flagellar, interphase, and mitotic microtubule dynamics in *Giardia* intestinalis. *Eukaryot Cell* 6:2354–2364.
47. Vidali L, Augustine RC, Kleinman KP, Bezanilla M (2007) Profilin is essential for tip growth in the moss Physcomitrella patens. *Plant Cell* 19:3705–3722.
48. Woods A, et al. (1989) Definition of individual components within the cytoskeleton of Trypanosoma brucei by a library of monoclonal antibodies. *J Cell Sci* 93:491–500.
49. Kane AV, Ward HD, Keusch GT, Pereira MEA (1991) In vitro encystation of *Giardia* lamblia: large-scale production of in vitro cysts and strain and clone differences in encystation efficiency. *J Parasitol* 77:974–981.
50. Ladwein M, Rottner K (2008) On the Rho'd: The regulation of membrane protrusions by Rho-GTPases. *FEBS Lett* 582:2066–2074.
51. Eggert US, Mitchison TJ, Field CM (2006) Animal cytokinesis: From parts list to mechanisms. *Annu Rev Biochem* 75:543–566.